Title: HSF1 excludes CD8+ T cells from breast tumors via suppression of CCL5.

Authors: Curteisha Jacobs[1], Sakhi Shah[1], Wen-Cheng Lu[1], Haimanti Ray[1], John Wang[1], Kenneth P. Nephew[3,4], Xin Lu[6], Sha Cao[4,5], *Richard L. Carpenter[1,2,4]

Affiliations: [1]Medical Sciences, Indiana University School of Medicine, Bloomington, IN, 47405, USA, [2]Department of Biochemistry and Molecular Biology, [3]Department of Anatomy, Cell Biology & Physiology, [4]Melvin and Bren Simon Comprehensive Cancer Center, [5]Department of Biostatistics and Health Data Science, Indiana University School of Medicine, Indianapolis, IN, 46202, USA. [6]Department of Biological Sciences, University of Notre Dame, Notre Dame, IN 46556, USA.

Running Title: HSF1 blocks CD8 T cells

Keywords: HSF1, CD8, T cells, breast cancer, CCL5

Additional Information:

*Corresponding Author Contact Information:
Address: 308 Biology Building, 1001 E. 3rd St., Bloomington, IN 47405
Email: richcarp@iu.edu
Phone: (812) 855-8214
Fax: (812) 855-4436

Conflict of Interest: The authors declare no potential conflicts of interest.

Manuscript Information:
Number of Figures:
Number of Supplemental Figures:
Word Count:

Abstract

Heat shock factor 1 (HSF1) is a stress-responsive transcription factor known to promote malignancy of several cancers, including breast cancer. To study the relationship of HSF1 activity to breast cancer phenotypes, we generated a 23-gene HSF1 Activity Signature (HAS) that accurately reports HSF1 transcriptional activity. This signature accurately reported previously known functions of HSF1, including response to heat stress, as well as HSF1 relationship to breast cancer. Namely, the HAS reported increased activity in tumors compared to normal and association with worse patient outcomes. This HAS gene set was used to assess the association of HSF1 activity with immune cell types in breast cancer. Interestingly, the HAS was negatively associated with the presence of CD8+ T cells in breast tumors, which was also observed in primary patient tumor specimens. Depletion of HSF1 in the immune-competent 4T1-Balb/c model led to decreased tumor volume, which was rescued with depletion of CD8+ T cells, suggesting HSF1 suppresses CD8+ T cells to prevent immune-mediated killing of breast cancer cells. Furthermore, loss of HSF1 also caused increased expression and secretion of the chemokine CCL5, a known recruiter of CD8+ T cells. Depletion of CCL5 prevented the attraction of CD8+ T cells observed with loss of HSF1. These data demonstrate a model whereby HSF1 suppresses CCL5, leading to less CD8+ T cells in breast tumors preventing immune-mediated destruction. This novel mechanism may contribute to the low levels of antitumor immune cells frequently observed in breast cancer and may also suggest inhibition of HSF1 as a therapeutic strategy to increase immune infiltration into breast tumors.

Introduction

Breast Cancer is the second leading cause of cancer related deaths in women with 1 in 8 developing invasive breast cancer over the course of their lifetime (1). Immune checkpoint therapy in breast cancer patients has had mixed results with triple-negative breast cancer (TNBC) patients primarily being the beneficiary of this therapeutic approach (2,3). Breast cancer has historically been thought to be a low immunogenic tumor with several results in the last decade supporting this notion of lower immune infiltration and lower tumor mutational burden compared to other cancer types (4,5). TNBC has largely benefitted from immune checkpoint therapy due to it being the small subset of breast cancer that has shown to have PD-L1 expression and higher lymphocytic infiltration relative to other breast cancer subtypes (6-9). Even though PD-L1-targeting checkpoint therapy is approved for high risk TNBC, only a small percentage of these patients respond to immune checkpoint inhibition. Previous studies have identified that higher lymphocyte infiltration in breast cancers is associated with improved survival and improved response to treatments (10-16). In particular, infiltration of CD8+ T cells, the primary cytotoxic lymphocyte, is an independent predictor of patient outcome and are trafficked to tumors through chemotactic cytokines (11). While low mutational burden is a significant factor in the low lymphocyte infiltration in breast cancer, it does not fully explain the low lymphocyte infiltration indicating there are additional mechanisms that suppress lymphocyte attraction to breast tumors.

Heat Shock Factor 1 (HSF1) is a master transcription factor regulator of the heat shock response with this classical function of HSF1 being to regulate expression of chaperone genes in response to cellular stressors (17-20). In breast cancer, HSF1 can be overexpressed with 10-15% of patients having HSF1 gene amplification (17). In addition, HSF1 can be hyperactivated stemming from increased proteotoxic stress and hyperactivation of activating kinases including AKT1, mTORC1, and p38 among others (21-25). A seminal finding describing the function of HSF1 in cancer identified that HSF1 has a unique transcriptional program in cancer cells, distinct from the heat stress response transcriptional program, that indicated HSF1 has several additional functions in cancer (26). These findings, along with many additional since, indicate HSF1 functions in cancer include promotion of epithelial-to-mesenchymal transition (21,27), promotion of the cancer stem-like state (28-30), promotion of cancer-associated metabolic changes (31,32), involvement in DNA repair (33), and several others that all support the malignancy of cancer cells. Because of its heavy involvement in these cancer-related processes, it is no surprise that HSF1 levels and activity have been associated with worsened patient outcomes in many cancer types, including breast cancer (26,34,35). While these studies have increased in our understanding of HSF1 biology in cancer over the last decade, the role of HSF1 in tumor-immune interactions remains unclear.

Gene signatures, or sets of genes that represent higher-level biological functions or features, have gained popularity since the first introduction of gene set enrichment analysis (GSEA) and an early version of the molecular signatures database (mSigDB) (36). A recent and significant update to the mSigDB now includes the gene transcription regulation database (GRTD) wherein a more integrated analysis that includes ChIP-Seq and RNA-Seq were utilized to develop gene sets that are more accurate for transcription factor function (37). However, the GRTD does not contain a gene set for HSF1 as of this report. Here we report a new HSF1 gene signatured termed "HSF1 Activity Signature," or HAS, which is a 23-gene signature that reports HSF1 transcriptional activity that was generated using a novel method of determining gene signatures. Using the HAS, we report a novel mechanism for breast tumor evasion of immune destruction whereby HSF1 suppresses recruitment of CD8+ T cells to tumors by suppressing expression and secretion of the CD8+ T cell chemokine CCL5.

Materials and Methods

Cell Culture and RNA-sequencing of Cell Lines: MDA-MB-231 and 4T1 cells were obtained from ATCC and were maintained at 37°C in 5% CO_2. MDA-MB-231 cells were cultured in DMEM (Gibco) and 4T1 were cultured in RPMI (Gibco) media supplemented with 10% fetal bovine serum (Corning) and 1% penicillin/streptomycin (Gibco). Cells were tested monthly for mycoplasma contamination using MycoAlert kit (Lonza). Lentiviral plasmids carrying control or HSF1 shRNA were synthesized by VectorBuilder using U6-driven promoter. MDA-MB-231 cells and 4T1 cells expressing control or HSF1-directed shRNA were subjected to lysis and total RNA collection using the PureLink RNA extraction kit with DNAse treatment (ThermoFisher). Total RNA was then subjected to mRNA-sequencing using an Illumina HiSeq 4000. Raw reads were processed and differential expression was performed as we have done previously (38).

Datasets Used: MCF7 and BPLER cells with HSF1 knockdown or heat shock were accessed from GSE38232. Hela cells with HSF1 knockdown and heat stress were accessed from GSE3697. A549 cells with heat shock were accessed from GSE83844. U2OS cells with heat shock were accessed from GSE115973. The breast cancer TCGA dataset was accessed through the TCGA data portal hosted by the Broad Institute. The METABRIC dataset was accessed through the European Genome-Phenome Archive (EGA) under study ID EGAS00000000083. The last breast cancer cohort was accessed from GSE47561.

Heat Map Generation and Principal Component Analysis: Expression from relevant samples were converted to z-scores for each gene within the respective signature gene lists. Z-scores were then used to generate heat maps using Morpheus (39). Gene expression values for the respective genes within each signature were subjected to principal component analysis using GraphPad Prism 9. PC1 scores for samples from respective groups were used to rank order samples for survival analysis or used to compare signature scores between groups using one-way ANOVA with Tukey post-hoc test (>2 groups for comparison) or students *t*-test (2 groups for comparison).

Gene Ontology (GO): Gene ontology analysis for the genes within the HAS or genes highly associated with the HAS using ShinyGO version 0.76 (40). Genes associated with the HAS were selected through pearson correlation of HAS score with all genes within the BRCA TCGA cohort and the top genes were subjected to gene ontology analyses. False discovery rate (FDR) and fold enrichment were used to determine significance of gene ontologies.

Survival Assessment: Patient survival was assessed using Kaplan-Meier plots within Prism 9. Log-Rank tests were used for determination of statistical differences between groups. Cox proportional hazard ratios were computed using PC1 scores from gene signatures with outcomes of overall survival, disease-free survival, or metastasis-free survival using SPSS 28.0 and calculated 95% confidence interval and computed p-values.

Gene Set Enrichment Analysis (GSEA): GSEA was done as previously described (28,41). Gene Cluster Text file (.gct) was generated from the TCGA BRCA, METABRIC, or GSE47561 breast cancer cohorts. Categorical class file (.cls) was generated by separating patients in these datasets based on high and low HAS score. The Gene Matrix file (.gmx) was generated using published gene signatures for immune cell types from CIBERSORT, TIMER, QuantiSeq, MCPCounter, and XCell (42). The number of permutations was set to 1000 and the chip platform for TCGA gene lists was used. Heat maps were generated using Normalized enrichment scores (NES).

Immune Profile Estimations: Immune proportion estimates were completed using deconvolution algorithms from TIMER, CIBERSORT, QuantiSeq, MCPCounter, and XCell for the TCGA-BRCA, METABRIC, and GSE47561 datasets using the TIMER2.0 portal (http://timer.cistrome.org). CD8+ T cell proportions were compared between high and low HAS groups using students t-test. CD8+ T cell proportions were also used to group patients into high HAS/Low CD8+ T cell, low HAS/high CD8+ T cell, and intermediate HAS/intermediate CD8+ T cell groups for survival analysis in all 3 breast cancer datasets.

Immunohistochemistry (IHC): IHC was performed on a breast cancer tumor microarray (BR1141A; US Biomax, now tissuearray.com effective 10/1/22). Antibodies used for IHC include pHSF1 (S326) (Abcam), CD3A (Santa Cruz), CD8A (CST), and CCL5 (Invitrogen). Tissue slides were deparaffinized in xylenes, rehydrated in successively lower ethanol solutions, quenching endogenous peroxidases with Bloxall (VectorLabs), followed by antigen retrieval according to antibody manufacturer recommendations. Antibody staining was developed with ABC-HRP kit (VectorLabs) and ImmPACT DAB kit (VectorLabs). Slides were imaged with Motic EasyScan scanner and analyzed with QuPath software (43) to assess number of positive cells, number of positive nuclei, and DAB intensity.

Animal Studies: Control or HSF1 knockdown 4T1 cells (3e5) were injected into the mammary gland of 4-week old Balb/c mice and allowed to growth for 4-5 weeks. Tumor volume was measured with calipers. When CD8+ T cells were depleted, mice were administered antibodies for Cd8a (bioXcell) as previously described (44). Briefly, mice were administered 200 ug of antibodies for 3 days to induce depletion. After induction, depletion was maintained throughout the study with 200 ug antibody injections twice per week. Spleens were collected for flow cytometry to confirm CD8+ T cell depletion after induction and at the end of the study. At the conclusion of the studies, tumors were extracted and subjected to paraffin embedding and IHC.

Flow Cytometry: Single cell suspensions were subjected to incubation with mouse-specific Cd3a (Miltenyi) and Cd8a (Miltenyi) antibodies in series followed by incubation with Zombie viability dye (Invitrogen). After labelling, flow cytometry was performed using a MACS Quant (Miltenyi) system and data were analyzed with FlowJo 10.8. Percentages of CD8+ T cells are graphed and were compared using one-way ANOVA with Tukey's post-hoc test or Students t-test where appropriate.

Cytokine Array: Control and HSF1 knockdown 4T1 cells were incubated in fresh media over 72 hours. Culture media was collected, centrifuged, and subjected to the Mouse XL Cytokine Array (R&D Systems) according to manufacturer's instructions. Experiment was performed with biological triplicates.

RT-qPCR: RNA was extracted from cells using an RNA isolation kit with DNAse treatment (Zymo). RNA was subjected to reverse transcription using RT Master Mix (Applied Biosystems). qPCR was performed with SYBR Green Master Mix (Applied Biosystems) using a QuantStudio 3 (Applied Biosystems). Experiments were performed in biological triplicate and analyzed using the ΔΔCt method. qPCR primers used include i) Mouse Ccl5 Forward: TGCCCACGTCAAGGAGTATTTC, Reverse: AACCCACTTCTTCTCTGGGTTG; ii) Mouse Actinb Forward: CACTGTCGAGTCGCGTCC, Reverse: CGCAGCGATATCGTCATCCA; iii) Human CCL5 Forward: GAGCGGGTGGGGTAGGATAGTGAGG, Reverse: CCACACCCTGCTGCTTTGCCTACAT; iv) Human ACTINB Forward: GCACAGAGCCTCGCCTT, Reverse: GTTGTCGACGACGAGCG.

Transwell Migration of T cells: Transwell migration was adapted from previous version (45). Briefly, the assay was performed using a chemotaxis chamber (NeuroProbe) with 5 μm pore size filters (NeuroProbe). Spleen were extracted from healthy Balb/c mice, dissociated using a gentleMACS and Spleen Isolation Kit (Miltenyi), and T cells isolated using a pan-T cell Isolation Kit (Miltenyi). T cells (1e6) were placed in the upper chamber in serum-free medium while the lower chamber contained serum-free medium with or without exogenous CCL5 or conditioned medium from 4T1 cells with pre-designed AccuTarget control siRNA, Hsf1 siRNA, or Ccl5 siRNA (Bioneer). T cells were incubated for 24 hours and subjected to flow cytometry with Cd3a/Cd8a antibodies to identify the counts of CD8+ T cells that migrated. Experiments were performed with 5 biological replicates.

Results

Identification of an HSF1 Activity Signature (HAS) that detects changes in HSF1 transcriptional activity.

HSF1 was originally discovered for its role as the master regulator of the heat shock response (18,20). The discovery of new functions of HSF1 has particularly been fruitful in the context of cancer where it has been found to regulate a target gene set that is distinct from the genes targeted by HSF1 in response to heat shock and play a role in many processes that promote malignancy (26,34). To better determine what cancer cell processes are associated with HSF1 transcriptional activity, we sought to identify a computational approach by which we could associate HSF1 transcriptional activity with cancer-related processes and with outcomes of cancer patients. HSF1 has a complex post-translational activation process whereby it must localize to the nucleus where it undergoes trimerization and DNA binding in addition to phosphorylation prior to recruiting general transcription factors to initiate transcription at target genes. Because of this complex activation process at the protein level, RNA levels of the HSF1 gene are not highly predictive for HSF1 transcriptional activity and do not significantly increase expression in response to heat shock (Suppl Fig. 1A-C). We reasoned that the most predictive gene set for HSF1 transcriptional activity will be RNA expression levels of genes that 1) are direct HSF1 target genes, 2) have high intra-gene correlation within the gene set across multiple datasets, 3) decrease expression when HSF1 is knocked down or inhibited, 4) increase expression in response to heat shock, and 5) show a trend of increased expression in cancer samples compared to normal. Therefore, we attempted to identify a set of genes that meet these criteria utilizing the gene selection procedures outlined in Figure 1A.

We first identified genes that are direct transcriptional targets of HSF1 utilizing more than 40 ChIP-Seq samples in the public domain (26,32,46). All unique genes included in the initial gene list as potential HSF1 target genes. To identify target genes from this initial list that are dependent on HSF1 for their expression, we removed genes from the initial list whose expression was not decreased with the knockdown of HSF1. The genes in this reduced gene set were then assessed for their correlation with every other gene in this gene set across 11 different cancer expression datasets to develop an adjacency matrix to identify subgroups of genes that have high intra-gene correlation. The adjacency matrix identified 9 different gene sets for consideration, which we determined the ability of these gene sets to detect changes in HSF1 transcriptional activity. One gene set, hereafter referred to as the HSF1 Activity Signature (HAS), was found to have the highest intra-gene correlation (Fig. 1B) and outperformed all other gene sets when HSF1 was knocked down in the presence or absence of heat shock (Fig. 1C, Suppl. Fig. 1D-K). The HAS gene set was also consistently decreased when HSF1 was knocked down in various cancer cell lines as well as the HSF1 inhibitor DTHIB (Fig. 1C-D; Suppl. Fig. 2A-C). Inversely, the HAS showed consistent increases after heat stress in various cell lines (Fig. 1C-E; Suppl. Fig. 2D-E). Principal component analysis (PCA) was performed and PC1 of the HAS accounted for 60-85% of the variance across these experiments (Suppl. Fig. 3A-G). To compare HAS across samples, PC1 for each sample was used to observe a significant decrease in samples with HSF1 knockdown and was also significantly increased in samples with heat shock (Suppl. Fig. 3A-G). The HAS consisted of 23 genes, which were analyzed with gene ontology that revealed several ontologies involved with protein folding, protein stabilization, heat shock proteins, unfolded proteins, chaperones, chaperonins, and chaperone complexes that were enriched (Suppl Fig. 1D-F) and indicative of the known function of HSF1 in proteostasis. The HSF1 binding motif was also the most enriched motif among the genes within the HAS (Suppl. Fig 1G). These data indicate the 23 gene set HAS, can reliably detect changes in HSF1 transcriptional activity.

HSF1 activity is associated with breast cancer patient outcomes and molecular characteristics.

HSF1 has previously been associated with several cancer phenotypes and increased expression and transcriptional activity in cancer cells (34). The HAS genes showed a clear increase in expression in tumor samples compared to matched normal adjacent tissue (Fig. 2A), indicating the HAS was able to detect an increase in HSF1 activity in tumors. We next assessed whether the HAS could serve as a biomarker for outcomes of breast cancer patients as previous studies show active HSF1 is associated with worse outcomes (26,30,35,46-48). First looking at overall survival, higher HAS was associated with worse overall survival in the TCGA breast cancer cohort (Fig. 2B) and the METABRIC breast cancer cohort (Fig. 2C) whereas expression of the HSF1 gene was not associated with overall survival in the TCGA cohort but was in the METABRIC cohort (Suppl. Fig. 6A-B). In addition to Kaplan Meier and Log Rank tests, age-adjusted hazard ratio for HAS was also significantly associated with worse overall survival in the TCGA (HR=2.42, 95% CI: 1.62-3.62; p<0.001) and the METABRIC (HR=1.58, 95% CI: 1.33-1.88; p<0.001) cohorts. The HAS was also associated with worse metastasis-free survival of breast cancer patients (Fig. 2D) whereas expression of the HSF1 gene was not significantly associated with metastasis-free survival (Suppl. Fig. 6C). HAS was also higher in tumors that eventually metastasized compared to tumors that never metastasized (Fig. 2E), further supporting a potential role for HSF1 in metastasis as previously suggested (26,28,49). These data indicate the HAS can predict breast cancer patient outcomes consistent with previous findings for HSF1 activity (26,28,35). These data indicate the HAS meet the criteria established above that this gene set has 1) direct HSF1 target genes, 2) high correlation within the gene set across multiple datasets, 3) decreased expression when HSF1 is knocked down or inhibited, 4) increase expression in response to heat shock, and 5) a trend of increased expression in cancer samples compared to normal.

We next assessed the relationship of the HAS with molecular subtypes of breast cancer. HAS was increased within the Luminal B (LumB), HER2-enriched (HER2-E), and Basal subtypes in both the METABRIC and TCGA cohorts compared to the Normal-Like (NL) and Luminal A (LumA) subtypes, which showed to be statistically significant when comparing PC1 of the HAS across these subtypes (Fig. 2F-G, Suppl. Fig. 4D-E). The HAS was also assessed in the METABRIC Integrated Clusters (IntClust) where it was observed that the HAS is upregulated in several integrated clusters that appear to mirror HAS activation from molecular subtypes. HAS was increased in IntClust 10 that is mostly associated with the basal molecular subtype, IntClust 5 that is closely associated with the HER2-enriched molecular subtype (Fig. 2H-I) (50). Interestingly, HAS was also elevated in clusters 1, 6, and 9 that are primarily ER-positive cancers that includes overlap with the LumB molecular subtype and possibly points towards an interaction between HSF1 and ERα, which a recent report identified HSF1 cooperates with ERα in breast cancer (51), and an interaction between HSF1 and HER2, which has been established (21,28,49,52-54). We next assessed the relevance of the HAS in other cancer types and it association with both disease-free survival and overall survival across the spectrum of TCGA cancer types (Fig. 3A-B). HSF1 has previously been associated with outcomes for many cancer types and the HAS reflected many of these known associations including liver (55,56), lung (57), pancreatic (58), melanoma (46), esophageal (48), cervical (59), and head/neck (60) cancers (Fig. 3A-B). The known roles of HSF1 in these various cancers illustrates its pleiotropic functions in cancer.

HSF1 Activity has a Negative Association with the Presence of CD8+ T cells in Breast Tumors.

Previous reports have indicated a possible association between HSF1 and tumor-immune interactions and immune function (26,61). However, this relationship has not been fully investigated or whether HSF1 has a functional effect on immune function or interaction with tumors. To investigate the relationship between HSF1 activity and tumor-immune interactions, the HAS was used to sort breast cancer patients into high and low HSF1 activity groups in the TCGA-BRCA (n=1100), METABRIC (n=1996), and GSE47561 (n=1570) cohorts. These groups were then subjected to gene set enrichment analysis (GSEA) to determine association of HSF1 activity with immune cell populations using multiple immune cell estimation algorithms (42,62-66). Interestingly, HSF1 activity was negatively associated with the presence of several immune cell types including CD8+ T cells, CD4+ T cells, and B cells across several different signatures for these cell types (Fig. 4A). Utilizing these algorithms to estimate immune cell proportions, it was consistently observed that patients with high HAS scores showed lower CD8+ T cells proportions compared to patients with low HAS scores (Fig. 4B-F). Furthermore, patients who had high HAS scores and low CD8+ T cells as estimated from CIBERSORT showed significantly worse overall survival or metastasis-free survival compared to patients with lower HAS and higher CD8+ T cell proportions (Fig. 4G-I). These data suggest that tumors with high HSF1 activity have lower CD8+ T cells and patients with this combination have worse outcomes. We next wanted to confirm these observations in primary patient specimens. Tumor tissues from a cohort of 114 breast cancer patients spanning all subtypes were subjected to IHC for the active mark of HSF1 (phosho-S326) that allowed us separate tumors into high or low HSF1 active tumors based on nuclear presence of p-HSF1 (Fig. 5A-B). These same specimens were co-stained with CD3A and CD8A antibodies to identify the CD8+ T cells. Similar to the computational results, these patient specimens had significantly less CD8+ T cells in tumors with high levels of active HSF1 (Fig. 5A, 5C). These data indicate a consistent relationship wherein tumors with high HSF1 activity have lower levels of CD8+ T cells.

HSF1 Functionally Affects the Level of CD8+ T cells in Breast Tumors.

While the negative relationship between HSF1 activity and the presence of CD8+ T cells was detected by association with computational approaches and assessment of patient specimens, it was unclear whether this relationship was a random association or a functional relationship. To test for a functional effect of HSF1 on CD8+ T cells, 4T1 cells were engineered to express control or HSF1-directed shRNA (Suppl. Fig. 5A). These cells were orthotopically grown in Balb/c mice for 3 weeks, after which it was confirmed that HSF1 expression was lost and resulted in a significantly smaller tumor volume (Fig. 6A, Suppl. Fig 5B). We further assessed the number of CD8+ T cells in these tumors with IHC and observed that tumors with HSF1 knockdown had significantly more CD8+ T cells compared to control tumors (Fig. 6B-C). These results suggest HSF1 may functionally regulate the attraction of CD8+ T cells to breast tumors. However, loss of HSF1 can also directly impact the cancer cells, which would lead to attraction of CD8+ T cells rather than an HSF1-driven control of CD8+ T cells. To determine the importance of CD8+ T cells to the loss of tumor volume after HSF1 knockdown, both control and HSF1 knockdown 4T1 cells were grown orthotopically in Balb/c mice with or without CD8+ T cell depletion by injection of CD8A antibodies. Splenic T cell counts confirmed that CD8+ T cells were indeed depleted at the end of the 3-week tumor growth period (Fig. 6D). Expectedly, depletion of CD8+ T cells led to increased tumor volume of control cells as CD8+ T cell depletion removes a tumor suppressor (Fig. 6E). Interestingly, CD8+ T cell depletion also rescued tumor growth for HSF1 knockdown tumors, which had a larger increase in tumor growth after CD8+ T cell depletion (~50 fold increase) compared to the increase in control tumors (~9 fold increase). The decrease in tumor volume with HSF1 knockdown coincided with an increase in CD8+ T cells whereas the depleted tumors showed near zero CD8+ T cells (Fig. 6F). These

results suggest that CD8+ T cells are a significant contributor to the loss of tumor volume with HSF1 knockdown and that HSF1 can protect breast tumors from immune-mediated killing.

HSF1 suppresses expression and secretion of CCL5, which is necessary to attract CD8+ T cells after HSF1 knockdown.

To understand how HSF1 activity in cancer cells results in suppression of CD8+ T cell infiltration into breast tumors, we tested whether HSF1 regulates secretion of cytokines that act as chemokines for CD8+ T cells. A cytokine array detecting over 100 cytokines was performed on conditioned media from 4T1 control and HSF1 knockdown cells. Interestingly, the cytokine that showed the second-largest increase with HSF1 knockdown was CCL5/RANTES (Fig. 7A), which is a canonical chemokine for CD8+ T cells (67). While this array measured secreted protein, the transcript levels of CCL5 from RNA-seq of control and HSF1 knockdown 4T1 cells showed similar increases with knockdown of HSF1, which was confirmed with qPCR in both mouse and human breast cancer cells (Fig. 7B-D). Inversely, overexpression of HSF1 decreased CCL5 transcript levels (Fig. 7E). HSF1 knockdown 4T1 tumors also showed an increase in CCL5 protein by IHC compared to control tumors (Fig. 7F). To test the importance of increased expression and secretion of CCL5 after HSF1 knockdown, transwell migration of T cells was tested (45). In this assay, general CD3+ T cells were isolated from Balb/c mice spleen and these T cells were placed in the upper chamber while the lower chamber contained chemokines or conditioned media and incubated for 24 hrs followed by assessment of the lower chamber by flow cytometry for CD3+/CD8+ T cells (Fig. 7G). Adding exogenous CCL5 to the lower chamber resulted in a directed migration of CD8+ T cells to the lower chamber indicating the assay is responding to a positive control (Fig. 7H). To test the effect of HSF1 loss, conditioned media from 4T1 cells with transient control or HSF1 siRNA were added the lower chamber of the T cell migration assay, which showed a significant increase in CD8+ T cell migration with HSF1 knockdown (Fig. 7I). Addition of CCL5 knockdown significantly reduced the CD8+ T cell migration observed with HSF1 only knockdown (Fig. 7I), suggesting the increased expression and secretion of CCL5 after HSF1 knockdown is necessary to attract CD8+ T cells. Taken together, these data suggest a model whereby tumors with high activity of HSF1 lead to suppression of CCL5 transcript and secreted protein that ultimately prevents attraction of CD8+ T cells toward breast tumors allowing the tumors to evade immune-mediate destruction (Fig. 7J).

Discussion

The major finding from these studies is activity of the stress response transcription factor HSF1 in breast cancer cells, known to support malignancy, repels CD8+ T cells away from breast tumors. Further, depletion of HSF1 resulted in an influx of CD8+ T cells that was found to be critical to reducing tumor volume after HSF1 depletion, thereby directly connecting HSF1 function to CD8+ T cells within breast tumors. While there has not been any previous direct connection established between HSF1 function within tumors and immune cell presence or infiltration, HSF1 gene expression was seen to be negatively associated with CD8+ T cell proportion estimates in breast cancer (61). Conversely, a recent report showed HSF1 can upregulate MHC proteins to enhance antigen presentation in the context of skin cancer, which would suggest high HSF1 activity would enhance attraction of CD8+ T cells and decrease tumor volume (68). The current study clearly indicates loss of HSF1 decreases tumor volume in an immune competent systems, which is consistent with previous results (49). Another report also suggests loss of HSF1 decreases cross-presentation of MHC class-I associated antigens (69). The current study and previous studies largely point to HSF1 functioning as an immune-suppressive factor in the context of cancer. These data further indicate for the first time that CD8+ T cells, specifically, are critical to the tumor suppressive effect of HSF1 depletion by regulating proportions of CD8+ T cells within breast tumors. These results would suggest that therapeutic targeting of HSF1 in breast tumors could lead to an influx of CD8+ T cells, which would enhance therapeutic response to several standard of care breast cancer therapies including taxanes and anthracyclines (13,70).

These results indicate the influx of CD8+ T cells after HSF1 depletion is due to an increase in CCL5 expression and secretion, suggesting CCL5 would serve a tumor suppressive function. However, the role of CCL5 in breast cancer is controversial as a recent report indicates CCL5 is associated with breast cancer metastasis (71). However, a previous report indicated therapeutic response to HDAC inhibitors in lung cancer is accompanied by a decrease in MYC function and an increase in CCL5 (72). The disparity in results for the function of CCL5 in cancer is puzzling but is likely related to expression of the CCL5 receptor, CCR5, on cancer cells. There is also precedent for an increase in cytokine-related signaling with HSF1 inhibition in other contexts, including listeria monocytogenes infection (73). Because these results saw a partial loss of CD8+ T cell attraction by silencing CCL5, it is likely that attraction of T cells after HSF1 depletion is regulated by additional mechanisms, including the aforementioned regulation of antigen presentation (69).

HSF1 has been known as the master regulator of the heat shock response since the mid-1980s (18,20). It was first observed to be altered in cancer in metastatic prostate cancer and has since been found to play a pleiotropic role in cancer where HSF1 can regulate many functions in cancer cells from metabolism to proliferation. Because of its many roles in cancer cells and across many cancer types, there is significant interest in studying HSF1, its activity, and its functions in cancer cells and identifying whether HSF1 activity has an impact on patient outcomes. Due to the complex activation of HSF1 protein activity, the transcript levels of HSF1 has poor utility in predicting or assessing HSF1 transcriptional activity. To this end, we developed here a gene signature, named HAS, that is comprised of 23 genes that are direct HSF1 gene targets and depend on HSF1 for their expression. Additionally, they have a high intra-gene correlation amongst these 23 genes such that increases in HSF1 activity largely result in the majority of the 23 genes to increase in expression. This gives an accurate and sensitive readout of HSF1 activity using transcript data, which was confirmed with studies wherein HSF1 gene was knocked down and wherein cells were exposed to heat shock, both of which have predictable effects on HSF1 activity. There is one previously reported HSF1 gene

signature, the CaSig, which was developed from elegant studies identifying many roles for HSF1 in cancer cells (26). While both the CaSig and HAS predict similar outcomes for cancer patients, the HAS does outperform the CaSig in measuring HSF1 transcriptional activity as measured by HSF1 knockdown or heat shock. The improved performance of the HAS in this instance is likely due to the intra-gene correlation as the CaSig (456 genes) had low intra-gene correlation. The application of the HAS will allow for future analysis of HSF1 transcriptional activity with cancer cell functions, patient outcomes, therapeutic response, and many others.

These studies indicate a novel mechanism regulating CD8+ T cell presence in breast tumors wherein hyperactive HSF1 suppresses CCL5 leading to decreased attraction of CD8+ T cells. Breast cancer is a low immunogenic tumor, which could partially be explained by the high basal activity of HSF1 in breast tumors. Further studies are need to identify if other mechanisms are important to the effect of HSF1 on CD8+ T cells. Additionally, studies are underway to test whether inhibition of HSF1 with small molecular inhibitors, such as DTHIB (74), can result in the same influx of CD8+ T cells, which could prime the targeting of HSF1 as a potential clinical approach to making breast cancer cells more immune cell-rich. Lastly, the role of HSF1 in CD8+ T cell activity or exhaustion warrants further investigation considering HSF1 has been reported to upregulate PD-L1 expression on cancer cells (75,76). These results generate several new lines of investigation for the role of HSF1 in new aspects of tumor biology and tumor-immune interactions.

Acknowledgements

References (≤ 50)

1. ACS. Cancer Facts & Figures 2022. Atlanta, GA2022.
2. Gaynor N, Crown J, Collins DM. Immune checkpoint inhibitors: Key trials and an emerging role in breast cancer. Semin Cancer Biol **2022**;79:44-57
3. Swoboda A, Nanda R. Immune Checkpoint Blockade for Breast Cancer. Cancer Treat Res **2018**;173:155-65
4. Papillon-Cavanagh S, Hopkins JF, Ramkissoon SH, Albacker LA, Walsh AM. Pan-cancer analysis of the effect of biopsy site on tumor mutational burden observations. Commun Med (Lond) **2021**;1:56
5. Yoshihara K, Shahmoradgoli M, Martínez E, Vegesna R, Kim H, Torres-Garcia W*, et al.* Inferring tumour purity and stromal and immune cell admixture from expression data. Nat Commun **2013**;4:2612
6. Jamiyan T, Kuroda H, Yamaguchi R, Nakazato Y, Noda S, Onozaki M*, et al.* Prognostic impact of a tumor-infiltrating lymphocyte subtype in triple negative cancer of the breast. Breast Cancer **2020**;27:880-92
7. Liu S, Lachapelle J, Leung S, Gao D, Foulkes WD, Nielsen TO. CD8+ lymphocyte infiltration is an independent favorable prognostic indicator in basal-like breast cancer. Breast Cancer Res **2012**;14:R48
8. Loi S, Drubay D, Adams S, Pruneri G, Francis PA, Lacroix-Triki M*, et al.* Tumor-Infiltrating Lymphocytes and Prognosis: A Pooled Individual Patient Analysis of Early-Stage Triple-Negative Breast Cancers. J Clin Oncol **2019**;37:559-69
9. Park JH, Jonas SF, Bataillon G, Criscitiello C, Salgado R, Loi S*, et al.* Prognostic value of tumor-infiltrating lymphocytes in patients with early-stage triple-negative breast cancers (TNBC) who did not receive adjuvant chemotherapy. Ann Oncol **2019**;30:1941-9
10. Dieci MV, Tsvetkova V, Orvieto E, Piacentini F, Ficarra G, Griguolo G*, et al.* Immune characterization of breast cancer metastases: prognostic implications. Breast Cancer Res **2018**;20:62
11. Ogiya R, Niikura N, Kumaki N, Bianchini G, Kitano S, Iwamoto T*, et al.* Comparison of tumor-infiltrating lymphocytes between primary and metastatic tumors in breast cancer patients. Cancer Sci **2016**;107:1730-5
12. Ali HR, Provenzano E, Dawson SJ, Blows FM, Liu B, Shah M*, et al.* Association between CD8+ T-cell infiltration and breast cancer survival in 12,439 patients. Ann Oncol **2014**;25:1536-43
13. Denkert C, Loibl S, Noske A, Roller M, Müller BM, Komor M*, et al.* Tumor-associated lymphocytes as an independent predictor of response to neoadjuvant chemotherapy in breast cancer. J Clin Oncol **2010**;28:105-13
14. Lee HJ, Seo JY, Ahn JH, Ahn SH, Gong G. Tumor-associated lymphocytes predict response to neoadjuvant chemotherapy in breast cancer patients. J Breast Cancer **2013**;16:32-9
15. Mahmoud SM, Paish EC, Powe DG, Macmillan RD, Grainge MJ, Lee AH*, et al.* Tumor-infiltrating CD8+ lymphocytes predict clinical outcome in breast cancer. J Clin Oncol **2011**;29:1949-55
16. Seo AN, Lee HJ, Kim EJ, Kim HJ, Jang MH, Lee HE*, et al.* Tumour-infiltrating CD8+ lymphocytes as an independent predictive factor for pathological complete response to primary systemic therapy in breast cancer. Br J Cancer **2013**;109:2705-13
17. Gomez-Pastor R, Burchfiel ET, Thiele DJ. Regulation of heat shock transcription factors and their roles in physiology and disease. Nat Rev Mol Cell Biol **2018**;19:4-19
18. Parker CS, Topol J. A Drosophila RNA polymerase II transcription factor contains a promoter-region-specific DNA-binding activity. Cell **1984**;36:357-69

19.   Ritossa F. A new puffing pattern induced by temperature shock and DNP in Drosophila. Experientia **1962**;18:571-3

20.   Topol J, Ruden DM, Parker CS. Sequences required for in vitro transcriptional activation of a Drosophila hsp 70 gene. Cell **1985**;42:527-37

21.   Carpenter RL, Paw I, Dewhirst MW, Lo HW. Akt phosphorylates and activates HSF-1 independent of heat shock, leading to Slug overexpression and epithelial-mesenchymal transition (EMT) of HER2-overexpressing breast cancer cells. Oncogene **2015**;34:546-57

22.   Chou SD, Prince T, Gong J, Calderwood SK. mTOR is essential for the proteotoxic stress response, HSF1 activation and heat shock protein synthesis. PLoS One **2012**;7:e39679

23.   Dayalan Naidu S, Sutherland C, Zhang Y, Risco A, de la Vega L, Caunt CJ*, et al.* Heat Shock Factor 1 Is a Substrate for p38 Mitogen-Activated Protein Kinases. Mol Cell Biol **2016**;36:2403-17

24.   Lu WC, Omari R, Ray H, Wang J, Williams I, Jacobs C*, et al.* AKT1 mediates multiple phosphorylation events that functionally promote HSF1 activation. Febs j **2022**;289:3876-93

25.   Su KH, Cao J, Tang Z, Dai S, He Y, Sampson SB*, et al.* HSF1 critically attunes proteotoxic stress sensing by mTORC1 to combat stress and promote growth. Nat Cell Biol **2016**;18:527-39

26.   Mendillo ML, Santagata S, Koeva M, Bell GW, Hu R, Tamimi RM*, et al.* HSF1 drives a transcriptional program distinct from heat shock to support highly malignant human cancers. Cell **2012**;150:549-62

27.   Powell CD, Paullin TR, Aoisa C, Menzie CJ, Ubaldini A, Westerheide SD. The Heat Shock Transcription Factor HSF1 Induces Ovarian Cancer Epithelial-Mesenchymal Transition in a 3D Spheroid Growth Model. PLoS One **2016**;11:e0168389

28.   Carpenter RL, Sirkisoon S, Zhu D, Rimkus T, Harrison A, Anderson A*, et al.* Combined inhibition of AKT and HSF1 suppresses breast cancer stem cells and tumor growth. Oncotarget **2017**;8:73947-63

29.   Dong Q, Xiu Y, Wang Y, Hodgson C, Borcherding N, Jordan C*, et al.* HSF1 is a driver of leukemia stem cell self-renewal in acute myeloid leukemia. Nat Commun **2022**;13:6107

30.   Yasuda K, Hirohashi Y, Mariya T, Murai A, Tabuchi Y, Kuroda T*, et al.* Phosphorylation of HSF1 at serine 326 residue is related to the maintenance of gynecologic cancer stem cells through expression of HSP27. Oncotarget **2017**;8:31540-53

31.   Eroglu B, Pang J, Jin X, Xi C, Moskophidis D, Mivechi NF. HSF1-Mediated Control of Cellular Energy Metabolism and mTORC1 Activation Drive Acute T-Cell Lymphoblastic Leukemia Progression. Mol Cancer Res **2020**;18:463-76

32.   Santagata S, Mendillo ML, Tang YC, Subramanian A, Perley CC, Roche SP*, et al.* Tight coordination of protein translation and HSF1 activation supports the anabolic malignant state. Science **2013**;341:1238303

33.   Fujimoto M, Takii R, Takaki E, Katiyar A, Nakato R, Shirahige K*, et al.* The HSF1-PARP13-PARP1 complex facilitates DNA repair and promotes mammary tumorigenesis. Nat Commun **2017**;8:1638

34.   Carpenter RL, Gokmen-Polar Y. HSF1 as a Cancer Biomarker and Therapeutic Target. Curr Cancer Drug Targets **2019**;19:515-24

35.   Santagata S, Hu R, Lin NU, Mendillo ML, Collins LC, Hankinson SE*, et al.* High levels of nuclear heat-shock factor 1 (HSF1) are associated with poor prognosis in breast cancer. Proc Natl Acad Sci U S A **2011**;108:18378-83

36.   Mootha VK, Lindgren CM, Eriksson KF, Subramanian A, Sihag S, Lehar J*, et al.* PGC-1alpha-responsive genes involved in oxidative phosphorylation are coordinately downregulated in human diabetes. Nat Genet **2003**;34:267-73

37.   Kolmykov S, Yevshin I, Kulyashov M, Sharipov R, Kondrakhin Y, Makeev VJ*, et al.* GTRD: an integrated view of transcription regulation. Nucleic Acids Res **2021**;49:D104-d11

38. Marino N, German R, Podicheti R, Rusch DB, Rockey P, Huang J, *et al.* Aberrant epigenetic and transcriptional events associated with breast cancer risk. Clin Epigenetics **2022**;14:21

39. BroadInstitute. 2022 08/09/2022. Morpheus. <https://software.broadinstitute.org/morpheus>. 08/09/2022.

40. Ge SX, Jung D, Yao R. ShinyGO: a graphical gene-set enrichment tool for animals and plants. Bioinformatics **2019**;36:2628-9

41. Subramanian A, Tamayo P, Mootha VK, Mukherjee S, Ebert BL, Gillette MA, *et al.* Gene set enrichment analysis: a knowledge-based approach for interpreting genome-wide expression profiles. Proc Natl Acad Sci U S A **2005**;102:15545-50

42. Li T, Fan J, Wang B, Traugh N, Chen Q, Liu JS, *et al.* TIMER: A Web Server for Comprehensive Analysis of Tumor-Infiltrating Immune Cells. Cancer Res **2017**;77:e108-e10

43. Bankhead P, Loughrey MB, Fernández JA, Dombrowski Y, McArt DG, Dunne PD, *et al.* QuPath: Open source software for digital pathology image analysis. Sci Rep **2017**;7:16878

44. Laky K, Kruisbeek AM. In Vivo Depletion of T Lymphocytes. Curr Protoc Immunol **2016**;113:4.1.-4.1.9

45. Zang YC, Samanta AK, Halder JB, Hong J, Tejada-Simon MV, Rivera VM, *et al.* Aberrant T cell migration toward RANTES and MIP-1 alpha in patients with multiple sclerosis. Overexpression of chemokine receptor CCR5. Brain **2000**;123 (Pt 9):1874-82

46. Kourtis N, Moubarak RS, Aranda-Orgilles B, Lui K, Aydin IT, Trimarchi T, *et al.* FBXW7 modulates cellular stress response and metastatic potential through HSF1 post-translational modification. Nat Cell Biol **2015**;17:322-32

47. Gökmen-Polar Y, Badve S. Upregulation of HSF1 in estrogen receptor positive breast cancer. Oncotarget **2016**;7:84239-45

48. Tsukao Y, Yamasaki M, Miyazaki Y, Makino T, Takahashi T, Kurokawa Y, *et al.* Overexpression of heat-shock factor 1 is associated with a poor prognosis in esophageal squamous cell carcinoma. Oncol Lett **2017**;13:1819-25

49. Xi C, Hu Y, Buckhaults P, Moskophidis D, Mivechi NF. Heat shock factor Hsf1 cooperates with ErbB2 (Her2/Neu) protein to promote mammary tumorigenesis and metastasis. J Biol Chem **2012**;287:35646-57

50. Curtis C, Shah SP, Chin SF, Turashvili G, Rueda OM, Dunning MJ, *et al.* The genomic and transcriptomic architecture of 2,000 breast tumours reveals novel subgroups. Nature **2012**;486:346-52

51. Vydra N, Janus P, Kus P, Stokowy T, Mrowiec K, Toma-Jonik A, *et al.* Heat shock factor 1 (HSF1) cooperates with estrogen receptor α (ERα) in the regulation of estrogen action in breast cancer cells. Elife **2021**;10

52. Meng L, Gabai VL, Sherman MY. Heat-shock transcription factor HSF1 has a critical role in human epidermal growth factor receptor-2-induced cellular transformation and tumorigenesis. Oncogene **2010**;29:5204-13

53. Moreno R, Banerjee S, Jackson AW, Quinn J, Baillie G, Dixon JE, *et al.* The stress-responsive kinase DYRK2 activates heat shock factor 1 promoting resistance to proteotoxic stress. Cell Death Differ **2021**;28:1563-78

54. Schulz R, Streller F, Scheel AH, Rüschoff J, Reinert MC, Dobbelstein M, *et al.* HER2/ErbB2 activates HSF1 and thereby controls HSP90 clients including MIF in HER2-overexpressing breast cancer. Cell Death Dis **2014**;5:e980

55. Cigliano A, Pilo MG, Li L, Latte G, Szydlowska M, Simile MM, *et al.* Deregulated c-Myc requires a functional HSF1 for experimental and human hepatocarcinogenesis. Oncotarget **2017**;8:90638-50

56. Jin X, Moskophidis D, Mivechi NF. Heat shock transcription factor 1 is a key determinant of HCC development by regulating hepatic steatosis and metabolic syndrome. Cell Metab **2011**;14:91-103

57. Lee S, Jung J, Lee YJ, Kim SK, Kim JA, Kim BK, *et al.* Targeting HSF1 as a Therapeutic Strategy for Multiple Mechanisms of EGFR Inhibitor Resistance in EGFR Mutant Non-Small-Cell Lung Cancer. Cancers (Basel) **2021**;13

58. Chen K, Qian W, Li J, Jiang Z, Cheng L, Yan B, *et al.* Loss of AMPK activation promotes the invasion and metastasis of pancreatic cancer through an HSF1-dependent pathway. Mol Oncol **2017**;11:1475-92

59. Shi X, Deng Z, Wang S, Zhao S, Xiao L, Zou J, *et al.* Increased HSF1 Promotes Infiltration and Metastasis in Cervical Cancer via Enhancing MTDH-VEGF-C Expression. Onco Targets Ther **2021**;14:1305-15

60. Ishiwata J, Kasamatsu A, Sakuma K, Iyoda M, Yamatoji M, Usukura K, *et al.* State of heat shock factor 1 expression as a putative diagnostic marker for oral squamous cell carcinoma. Int J Oncol **2012**;40:47-52

61. Chen F, Fan Y, Cao P, Liu B, Hou J, Zhang B, *et al.* Pan-Cancer Analysis of the Prognostic and Immunological Role of HSF1: A Potential Target for Survival and Immunotherapy. Oxid Med Cell Longev **2021**;2021:5551036

62. Aran D, Hu Z, Butte AJ. xCell: digitally portraying the tissue cellular heterogeneity landscape. Genome Biology **2017**;18:220

63. Becht E, Giraldo NA, Lacroix L, Buttard B, Elarouci N, Petitprez F, *et al.* Estimating the population abundance of tissue-infiltrating immune and stromal cell populations using gene expression. Genome Biology **2016**;17:218

64. Finotello F, Mayer C, Plattner C, Laschober G, Rieder D, Hackl H, *et al.* Molecular and pharmacological modulators of the tumor immune contexture revealed by deconvolution of RNA-seq data. Genome Medicine **2019**;11:34

65. Newman AM, Steen CB, Liu CL, Gentles AJ, Chaudhuri AA, Scherer F, *et al.* Determining cell type abundance and expression from bulk tissues with digital cytometry. Nature Biotechnology **2019**;37:773-82

66. Li T, Fu J, Zeng Z, Cohen D, Li J, Chen Q, *et al.* TIMER2.0 for analysis of tumor-infiltrating immune cells. Nucleic Acids Research **2020**;48:W509-W14

67. Roussot N, Ghiringhelli F, Rébé C. Tumor Immunogenic Cell Death as a Mediator of Intratumor CD8 T-Cell Recruitment. Cells **2022**;11:3672

68. Li G, Kryczek I, Nam J, Li X, Li S, Li J, *et al.* LIMIT is an immunogenic lncRNA in cancer immunity and immunotherapy. Nat Cell Biol **2021**;23:526-37

69. Zheng H, Li Z. Cutting edge: cross-presentation of cell-associated antigens to MHC class I molecule is regulated by a major transcription factor for heat shock proteins. J Immunol **2004**;173:5929-33

70. Denkert C, von Minckwitz G, Darb-Esfahani S, Lederer B, Heppner BI, Weber KE, *et al.* Tumour-infiltrating lymphocytes and prognosis in different subtypes of breast cancer: a pooled analysis of 3771 patients treated with neoadjuvant therapy. Lancet Oncol **2018**;19:40-50

71. Qiu J, Xu L, Zeng X, Wu H, Liang F, Lv Q, *et al.* CCL5 mediates breast cancer metastasis and prognosis through CCR5/Treg cells. Front Oncol **2022**;12:972383

72. Topper MJ, Vaz M, Chiappinelli KB, DeStefano Shields CE, Niknafs N, Yen RC, *et al.* Epigenetic Therapy Ties MYC Depletion to Reversing Immune Evasion and Treating Lung Cancer. Cell **2017**;171:1284-300.e21

73.   Murapa P, Ward MR, Gandhapudi SK, Woodward JG, D'Orazio SE. Heat shock factor 1 protects mice from rapid death during Listeria monocytogenes infection by regulating expression of tumor necrosis factor alpha during fever. Infect Immun **2011**;79:177-84

74.   Dong B, Jaeger AM, Hughes PF, Loiselle DR, Hauck JS, Fu Y*, et al.* Targeting therapy-resistant prostate cancer via a direct inhibitor of the human heat shock transcription factor 1. Sci Transl Med **2020**;12

75.   Sasaya T, Kubo T, Murata K, Mizue Y, Sasaki K, Yanagawa J*, et al.* Cisplatin-induced HSF1-HSP90 axis enhances the expression of functional PD-L1 in oral squamous cell carcinoma. Cancer Med **2022**

76.   Yang T, Ren C, Lu C, Qiao P, Han X, Wang L*, et al.* Phosphorylation of HSF1 by PIM2 Induces PD-L1 Expression and Promotes Tumor Growth in Breast Cancer. Cancer Res **2019**;79:5233-44

Figure Legends

Figure 1: Identification of the HSF1 Activity Signature (HAS). A) The schema for identifying an HSF1 activity signature, which included input data from ChIP-Seq data to identify direct targets followed by removing genes not dependent on HSF1 and generating gene sets that have high intragene correlation. B) Correlation matrix of the 23-gene HAS across 11 cancer datasets. C-E) Heat maps were generated from publicly-available expression data from Hela cells with HSF1 knockdown and/or heat stress (C), MDA-MB-231 cells with or without HSF1 knockdown (D), and A549 cells with or without heat stress (E).

Figure 2: HAS is associated with breast cancer outcomes and molecular subtypes. A) Heat map was generated using matched adjacent normal and tumor expression data from the TCGA-BRCA cohort (n=100). B-D) Patients in the TCGA-BRCA (B), METABRIC (C), and GSE47561 (D) cohorts were sorted by their HAS scores and Kaplan-Meier plots were generated for overall survival (B-C) or metastasis-free survival (D). E) HAS PC1 scores for patients from GSE47561 with or without eventual metastasis. F) Heat map was generated for the HAS of the METABRIC cohort delineated by subtype. G) HAS PC1 scores were plotted and compared across subtypes via one-way ANOVA with Tukey's post-hoc test. H) Heat map was generated for the HAS of the METABRIC cohort delineated by METABRIC Clusters. I) HAS PC1 scores were plotting and compared across METABRIC Clusters and compared across clusters via one-way ANOVA with Tukey's post-hoc test.

Figure 3: Association of HAS with Outcomes Across TCGA Cancer Types. A-B) Cox hazard ratios were calculated for HAS, adjusted for age, across the TCGA cancer types for Disease-Free Survival (A) and Overall Survival (B). Forest plots were generated with hazard ratios (black square) with 95% confidence intervals (red bars).

Figure 4: HAS is Negatively Associated with Presence of CD8+ T cells. A) GSEA was performed in TCGA-BRCA, METABRIC, and GSE47561 cohorts with patients separated into high or low HAS scores. Signatures for immune cell types were assessed for enrichment with high or low HAS patients. Normalized enrichment scores (NES) are plotted on heat map. B-F) CD8+ T cell proportions were estimated in the TCGA-BRCA cohort using TIMER (B), CIBERSORT (C), QuantiSeq (D), MCPCounter (E), and XCell (F). CD8+ proportions are plotted in the high and low HAS patients. G-I) Patients in the TCGA-BRCA (G), METABRIC (H), and GSE47561 (I) cohorts were separated HAS scores and CD8+ T cell proportions estimated by CIBERSORT and Kaplan-Meier graphs were plotted for patient outcomes.

Figure 5: Active HSF1 in Breast Cancer Tumor Specimens Coincides with Low CD8+ T cells. A) A cohort of 114 breast tumors were subjected to IHC with antibodies for CD3A, CD8A, and pHSF1 (S326). B) Patients were separated into high or low HSF1 active tumors based on nuclear positivity percentage for pHSF1. C) CD8+ T cells assessed by CD3+/CD8+ cells are plotted for the high or low HSF1 active tumors.

Figure 6: HSF1 Functionally Regulates the Amount of CD8+ T cells in Breast Tumors. A) 4T1 cells (5e4 cells) with or without HSF1 knockdown were grown orthotopically in Balb/c mice for 3 weeks. Tumor volume at the conclusion of the study is graphed. B) IHC was performed on tumors from (A) for CD8A to identify CD8+ T cells. C) CD8+ T cells from (B) was quantified for control and HSF1 knockdown tumors. D) Balb/c mice were given either PBS control or CD8A antibodies to deplete CD8+ T cells in vivo. Control and HSF1 knockdown cells were then grown orthotopically for 3 weeks. Spleen were collected at the conclusion of the study, dissociated, and cells were subjected to flow cytometry to confirm the depletion of CD8+ T cells. E) Tumor

volume at the conclusion of the study from (D) is plotted. F) Tumor tissue from (D) was subjected to IHC for CD8A to assess the CD8+ T cells.

Figure 7: HSF1 suppresses CCL5 to prevent attraction of CD8+ T cells. A) Conditioned media was grown for 72 hours on control or HSF1 knockdown 4T1 cells. Conditioned media was then subjected to a cytokine array detecting over 100 cytokines. The cytokines increased with HSF1 knockdown are listed. B) CCL5 mRNA levels in control and HSF1 knockdown 4T1 cells assessed by RNA-Seq. C) CCL5 mRNA levels in control and HSF1 knockdown 4T1 cells assessed by RT-qPCR. D) CCL5 mRNA levels in control and HSF1 knockdown MDA-MB-231 cells assessed by RT-qPCR. E) CCL5 mRNA levels in MDA-MB-231 cells expressing empty vector or HSF1 assessed by RT-qPCR. F) IHC of CCL5 in 4T1 control and HSF1 knockdown tumors from Fig. 6A. G) Schematic of T cell transwell migration assay wherein pan-T cells were incubated in the upper chamber for 24 hours with conditioned media in the lower chamber, after which the lower chamber was subjected to flow cytometry to detect CD8+ T cells. H) Adding exogenous CCL5 to the lower chamber of the T cell transwell migration assay led to CD8+ T cell migration. I) Conditioned media from 4T1 cells expressing either control, HSF1, or HSF1+CCL5 siRNA were placed in the lower chamber for the T cell transwell migration assay. CD8+ T cell proportions are plotted for each group (n=5). J) Model indicating HSF1 suppresses CCL5 expression and secretion leading to decreased attraction of CD8+ T cells toward breast cancer cells.
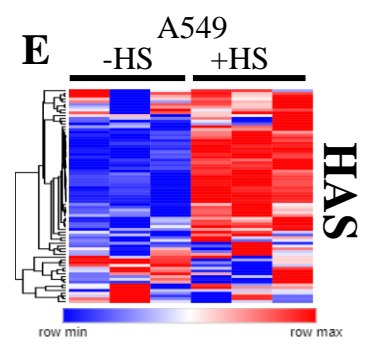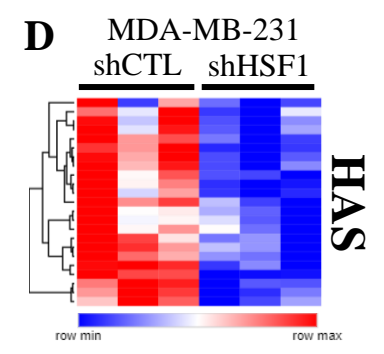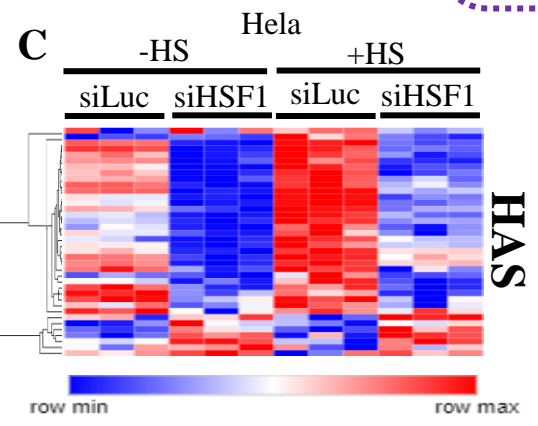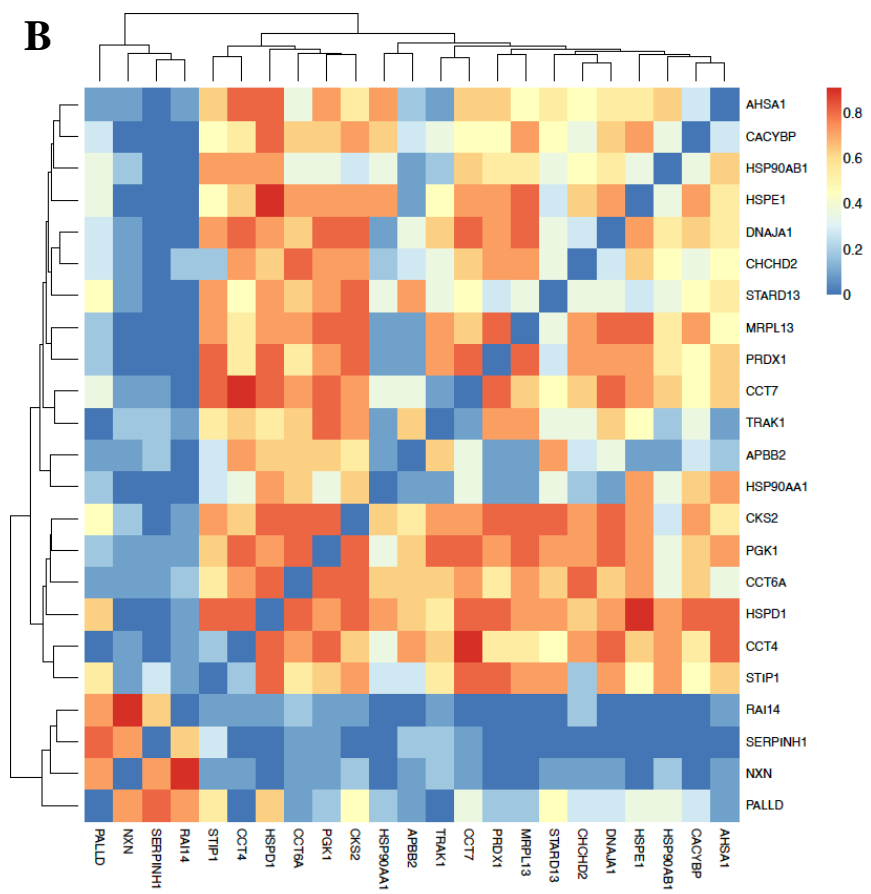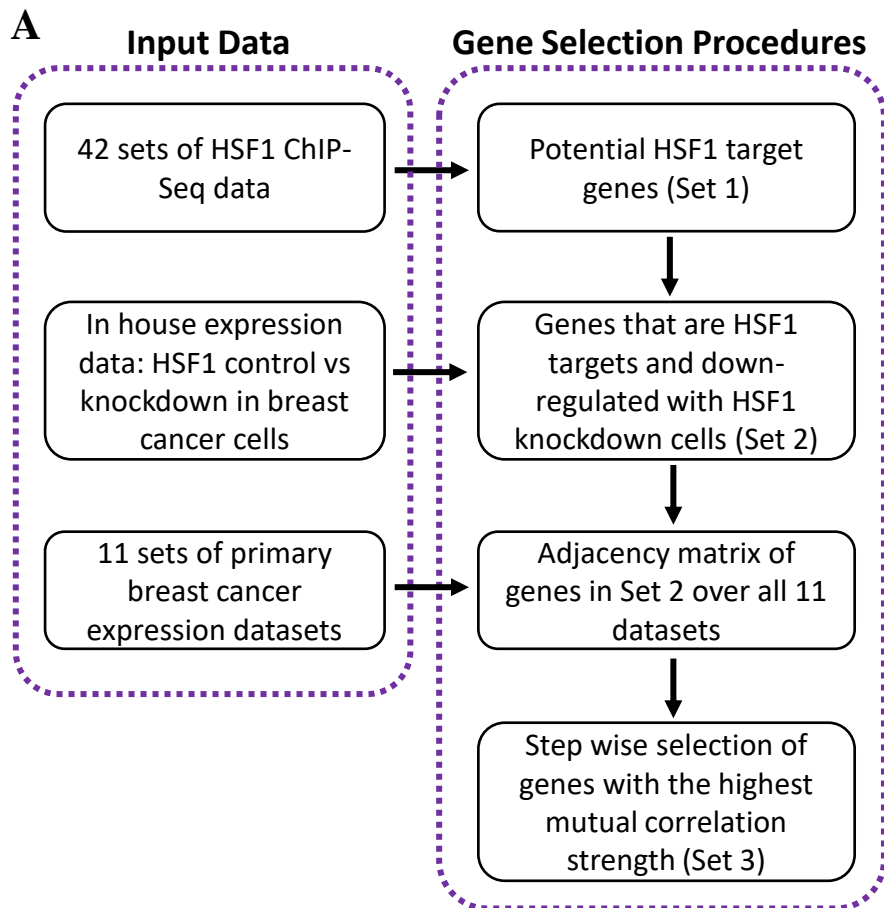
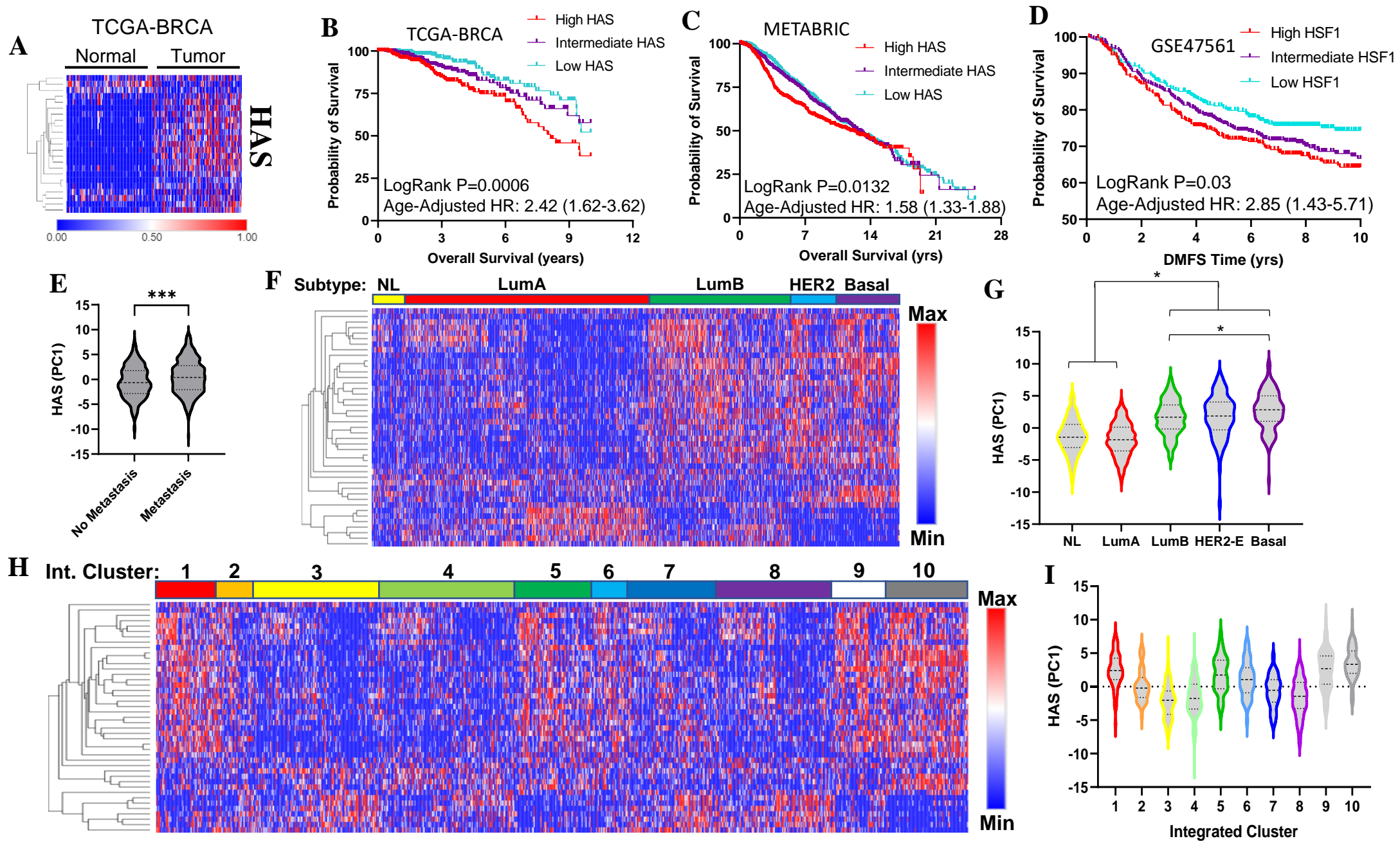Figure 1: Identification of the HSF1 Activity Signature (HAS).

Figure 2: HAS is associated with specific breast cancer subtypes and patient outcomes.
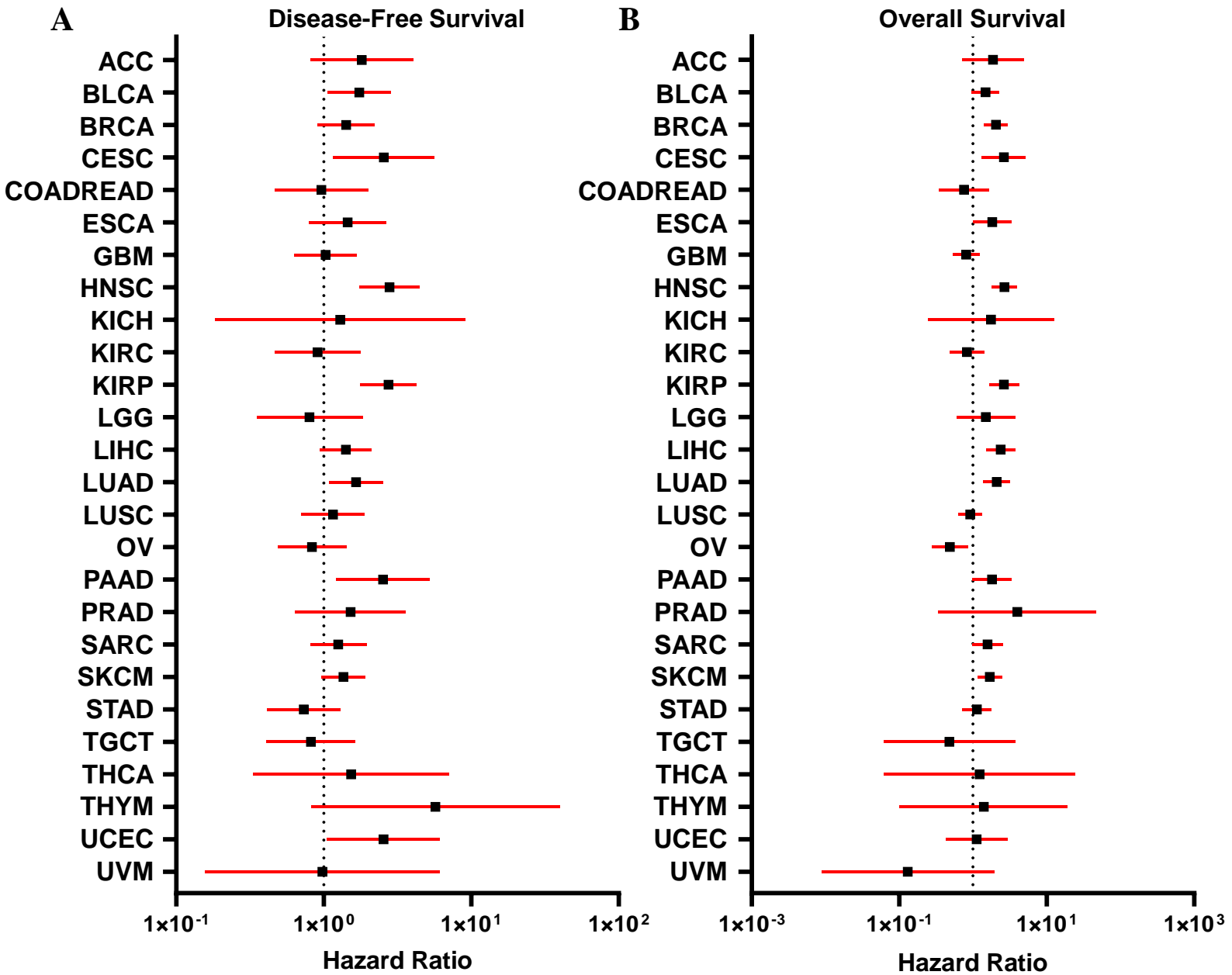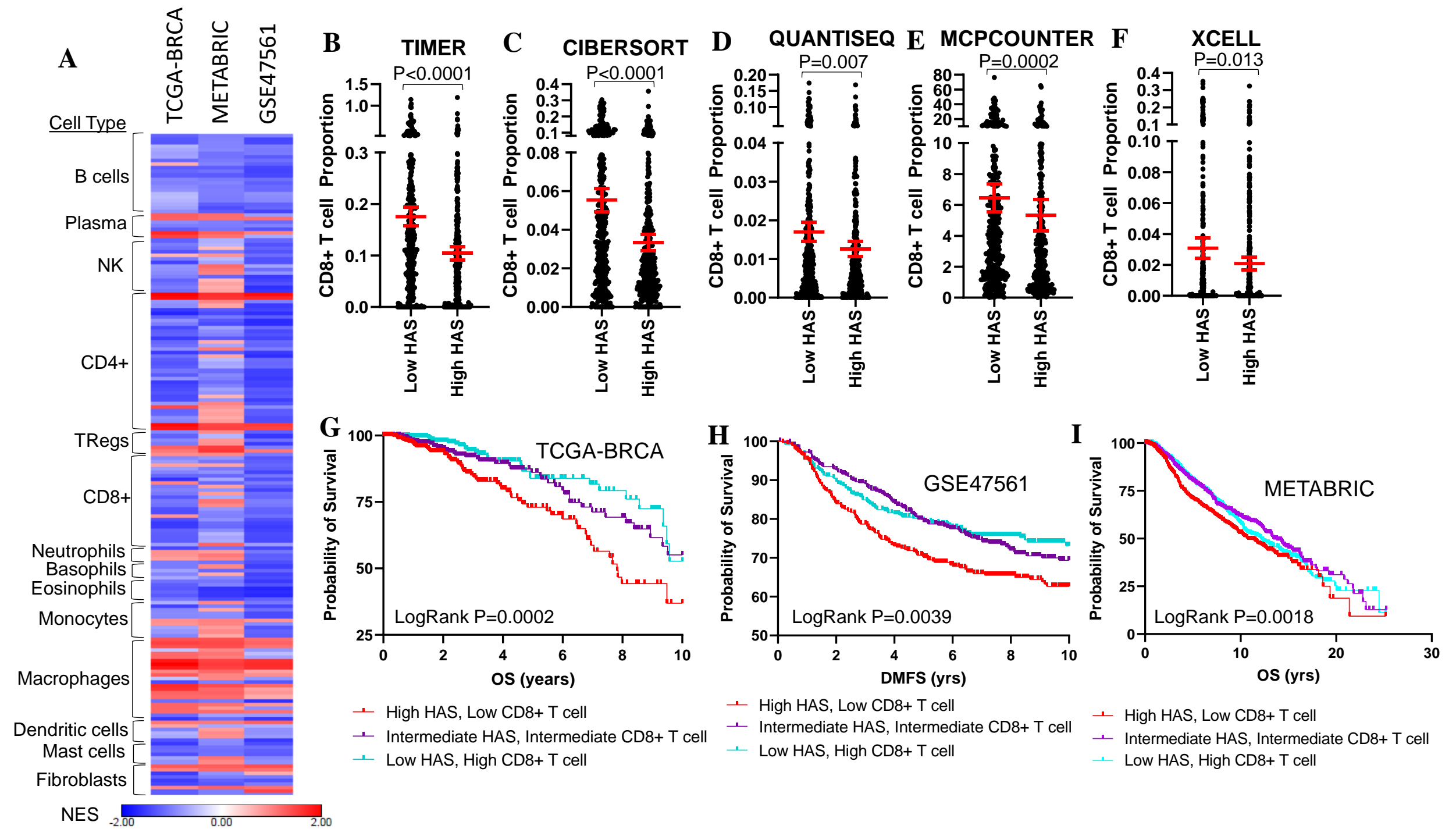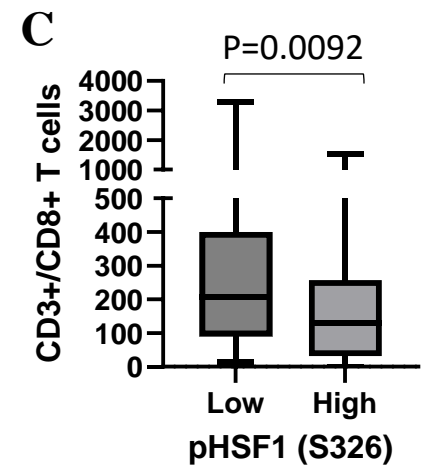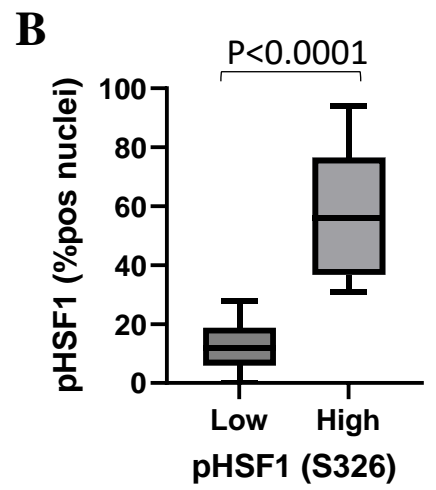
Figure 3: Association of HAS with Outcomes Across Cancer Types
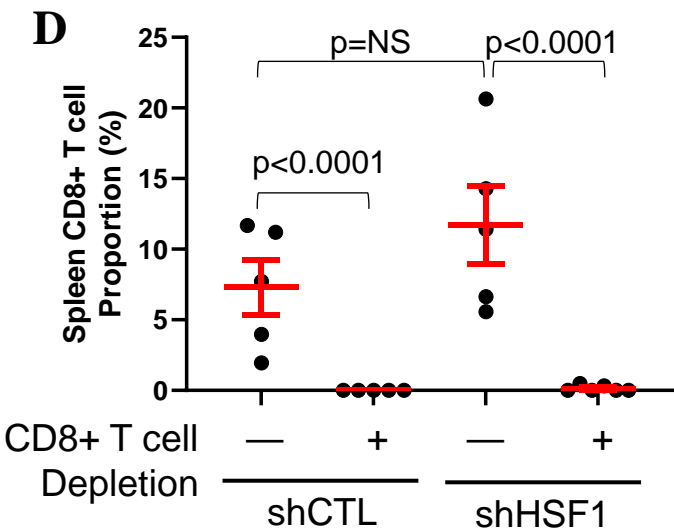
A

	High Nuclear pHSF1 Low CD3/CD8 T cell	Low Nuclear pHSF1 High CD3/CD8 T cell
CD3a/CD8a		
pHSF1 (S326)		

B

P<0.0001

pHSF1 (%pos nuclei)

Low   High
pHSF1 (S326)

C

P=0.0092

CD3+/CD8+ T cells

Low   High
pHSF1 (S326)

A

Tumor Volume (mm³)

P<0.001

shCTL shHSF1

B

shCTL shHSF1

CD8A

80um 80um

80um 80um

C

CD8+ T cells (#/field)

P<0.01

shCTL shHSF1

D

Spleen CD8+ T cell Proportion (%)

p=NS p<0.0001

p<0.0001

CD8+ T cell Depletion   − +   − +

shCTL   shHSF1

E

Tumor Volume (mm³)

p<0.0001

9.5 Fold

50.1 Fold

p<0.0001

CD8+ T cell Depletion   − +   − +

shCTL   shHSF1

F

CD8A

No Depletion   CD8 Depletion   No Depletion   CD8 Depletion

shCTL   shHSF1

A

Cytokine	Fold Change	P
MMP-9	6.6	0.0006
CCL5/RANTES	3.8	0.02
LIF	3.0	0.02
Pentraxin	2.4	0.2
Serpin	2.2	0.05
WISP-1/CCN5	2.0	0.1
IL-28	1.9	0.7
CXCL16	1.17	0.3
Osteopontin	1.1	0.5